The β Subunit Increases Ca^{2+} Currents and Gating Charge Movements of Human Cardiac L-Type Ca^{2+} Channels

Ira R. Josephson* and Gyula Varadi‡
*Department of Molecular and Cellular Physiology and ‡Institute of Molecular Pharmacology and Biophysics University of Cincinnati, College of Medicine, Cincinnati, Ohio 45267-0576 USA

ABSTRACT The properties of the gating currents (nonlinear charge movements) of human cardiac L-type Ca^{2+} channels and their relationship to the activation of the Ca^{2+} channel (ionic) currents were studied using a mammalian expression system. Cloned human cardiac α_1 + rabbit α_2 subunits or human cardiac α_1 + rabbit α_2 + human β_3 subunits were transiently expressed in HEK293 cells. The maximum Ca^{2+} current density increased from -3.9 ± 0.9 pA/pF for the $\alpha_1 + \alpha_2$ subunits to -11.6 ± 2.2 pA/pF for $\alpha_1 + \alpha_2 + \beta_3$ subunits. Calcium channel gating currents were recorded after the addition of 5 mM Co^{2+}, using a −P/5 protocol. The maximum nonlinear charge movement (Q_{max}) increased from 2.5 ± 0.3 nC/μF for $\alpha_1 + \alpha_2$ subunit to 12.1 ± 0.3 nC/μF for $\alpha_1 + \alpha_2 + \beta_3$ subunit expression. The Q_{ON} was equal to the Q_{OFF} for both subunit combinations. The Q_{ON}-V_m data were fit by a sum of two Boltzmann expressions and ranged over more negative potentials, as compared with the voltage dependence for activation of the Ca^{2+} conductance. We conclude that 1) the β subunit increases the number of functional α_1 subunits expressed in the plasma membrane of these cells and 2) the voltage-dependent activation of the human cardiac L-type calcium channel involves the movements of at least two nonidentical and functionally distinct gating structures.

INTRODUCTION

Cardiac L-type Ca^{2+} channels perform a central role in the electrical and contractile function of the heart, and their properties and regulation have been the focus of intensive investigation over the last several decades. Biochemical studies have revealed that the cardiac L-type Ca^{2+} channel is a heterotetrameric complex composed of α_1, α_2/δ, and β polypeptide subunits (Catterall, 1988; Kuniyasu et al., 1992; De Waard et al., 1994; Pragnell et al., 1994; Varadi et al., 1995). Recently the molecular structure of the human α_1 subunit, which forms the pore and contains the voltage-sensing structures of the cardiac L-type Ca^{2+} channel, has also been elucidated (Schultz et al., 1993). It has been proposed that the accessory subunits of the L-type calcium channel may regulate the gating kinetics and the density of calcium channel expression (see Isom et al., 1994). In addition, it was shown that the β subunit binding site is conserved for all calcium channel α_1 subunits and is located in the I-II cytoplasmic linker region (Pragnell et al., 1994). Similarly, the interaction site was mapped on the β subunit (De Waard et al., 1994), and it has been assigned to a 30-amino acid conserved domain at the amino terminus of the β subunit.

The Ca^{2+} channel subunits can be expressed in mammalian cell lines (Lory et al., 1993; Welling et al., 1993; Hofmann et al., 1994; Perez-Garcia et al., 1995) in which the cardiac Ca^{2+} channel currents can be studied by the application of the patch voltage-clamp method (Hamill et al., 1981). Using these methods it is possible to record ionic currents flowing through the cloned cardiac L-type Ca^{2+} channels. More importantly, the gating charge movements that govern the opening and closing of voltage-dependent L-type Ca^{2+} channels can be quantified, as has previously been demonstrated for native cardiac myocytes (Bean and Rios, 1989; Hadley and Lederer, 1989, 1991; Josephson and Sperelakis, 1992). Here we report the properties of the gating charge movements (gating currents) of human cardiac L-type Ca^{2+} channels composed of $\alpha_1 + \alpha_2$ or $\alpha_1 + \alpha_2 + \beta$ subunits and their relationship to the activation of the Ca^{2+} conductance.

MATERIALS AND METHODS

Cloning and cell transfection

Isolation of the Hb_3 cDNA clone

Polymerase chain reaction was used to isolate a clone encoding the β_3 subunit from human cardiac mRNA (Klockner et al., 1995). The sequence was found to be identical to that published by Collin et al. (1994).

Construction of expression plasmids in pAGS-3 vector

The coding region of the human cardiac α_1 clone (Schultz et al., 1993) (human heart-1) was removed using *Hin*dIII (5′-polylinker site) and *Hpa*I (8046) cleavages, whereas the pAGS-3 vector (Miyazaki et al., 1989) was cut with *Not*I (polylinker) and filled in with the Klenow fragment of DNA polymerase I to produce blunt ends then cut with *Hin*dIII (polylinker). The fragments were ligated and the construct was verified by restriction analysis. The skeletal muscle α_2 clone (Ellis et al., 1988) as well as the Hb_3 clone were transferred to pAGS-3 using *Hin*dIII/*Not*I sites. The resultant expression plasmids were verified by restriction mapping.

Received for publication 5 July 1995 and in final form 18 December 1995.
Address reprint requests to Dr. Ira R. Josephson, Department of Molecular and Cellular Physiology, University of Cincinnati, College of Medicine, Cincinnati, OH 45267-0576. Tel.: 513-558-3110; Fax: 513-558-5738; E-mail: josephson@uc.edu.

0006-3495/96/03/1285/09 $2.00

Transient expression

For the transient expression of the hHTα_1, α_2, and Hb_3 subunit, cDNA expression plasmids were transfected by the Ca^{2+}-phosphate method (Chen and Okayama, 1987) into HEK293 cells in a molar ratio of 1:2:3, respectively. Electrophysiological recordings were done 24–72 h after transfection of the HEK293 cells.

Monitoring the efficiency of transient transfections

Transient transfections were done in HEK293 cells (CRL1573; ATCC, Rockville, MD) using the Chen-Okayama procedure (Chen and Okayama, 1987). The efficiency of transfection was routinely monitored by cotransfection with the *E. coli* galactosidase gene (pCH110 plasmid; Pharmacia, Piscataway, NJ). The expression of the reporter gene was visualized either by histochemical staining (Sanes et al., 1986) or by fluorescent substrate according to the manufacturer's protocol (Molecular Probes, Eugene, OR). The transfection efficiency was assessed as the percentage of transfected cells and was found to be 41.1 ± 3.4% in 11 independently conducted experiments.

Electrophysiological recording

Ionic and nonlinear capacity currents were recorded using methods described previously (Josephson and Sperelakis, 1992). Single HEK293 cells were voltage-clamped using the whole-cell configuration of the patch-clamp technique (Hamill et al., 1981). Electrodes were fabricated from thin-wall borosilicate glass (TW-150; WPI Instruments, New Haven, CT) and filled with the following solution (in mM): CsOH, 120; glutamic acid, 120; $MgCl_2$, 2; Na_2 GTP, 0.2; Na_2 ATP, 2; EGTA, 10; HEPES buffer, 10. The pH was adjusted with HEPES to 7.25. The extracellular solution contained (in mM) NaCl, 140; KCl, 5.4; $MgCl_2$, 1; $CaCl_2$, 1.8, glucose, 10; HEPES, 10. The pH was adjusted to 7.4 with Trizma base. The electrode resistances ranged from 1 to 3 MΩ when filled with the electrode solution. Junction potentials were nulled before seal formation and no further corrections were made during the experiment. The seal resistances ranged between 10 and 50 gΩ.

In experiments designed to examine nonlinear charge movement all ionic currents were blocked. In addition to the internal Cs^+ solution, 5 mM Cs^+ was added to the external solution (to block the delayed outward K^+ currents). Tetrodotoxin (10 mM) was added to the external solution to block a small endogenous sodium current (present in a small percentage of the cells), and $CoCl_2$ (5 mM) was added to block the calcium channels.

Membrane currents were recorded using an Axopatch IB patch clamp (Axon Instruments, Burlingame, CA). Linear capacity current, due to the charging and discharging of the cell membrane capacitance, was suppressed by analog capacitance compensation. Careful attention to this procedure was necessary to prevent amplifier saturation due to the large amplitude of the capacity currents during rapid membrane charging. The series resistance and capacitance compensation adjustments were periodically monitored during each experiment, and the experiment was terminated if either parameter changed significantly (>5%).

Data acquisition and analysis

Data acquisition and analysis were performed using the PCLAMP programs (Axon Instruments) on an IBM AT computer. Membrane currents were filtered at a corner frequency of 10 kHz, amplified ten times with an eight-pole Bessel filter (Frequency Devices, Haverhill, MA), and digitized at 12 μs/point using a 12-bit A-D converter (Labmaster; Axon Instruments). To remove the residual linear capacity and leakage current components in the test current, five scaled, hyperpolarizing control voltage steps (each one-fifth the magnitude of the corresponding test step) were given from control subtracting holding potentials (SHPs) of −100 mV (−P/5), and the resulting summed control currents were added to the test currents. The linearity of the entire recording system was checked before experimentation by using an RC cell model circuit, and the −P/5 protocol yielded a zero current trace over the range of ±200 mV.

Sequences of test potentials were applied at a frequency of 0.5 Hz. This frequency allowed for complete recovery of charge, using the protocols described (determined by comparison of individual current recordings with the first recording in the average), and the current signals at each potential were averaged four times to improve the signal-to-noise ratio. Series of runs were bracketed (i.e., the original protocol was repeated) to ensure the stability of the currents over time, and the currents were not analyzed if a significant change (>5%) had occurred in either their magnitude or time course.

Steady-state integration measurements were performed on the ON and OFF currents (IgON and IgOFF). The ON and the OFF currents were integrated over the entire 5.4-ms voltage step using a baseline calculated from the mean (zero) current at the end of the trace (from 4.4 to 5.4 ms). In some experiments, the first few digitized points (30–150 μs) after the voltage step were imperfectly subtracted and they were not included in the charge integral. The voltage dependence for the charge movement (integrated at each test potential) was fitted with a sum of two Boltzmann expressions.

The currents are displayed after digital filtering in the figures. All experiments were conducted at a temperature of 20–23°C. Grouped data are presented as means ± SE, unless otherwise noted. A Student's *t*-test was used to determine whether the group data were significantly different.

RESULTS

Human cardiac calcium channel ionic currents

Representative examples of calcium channel currents (with a physiological concentration of Ca^{2+} ions (1.8 mM) as the charge carrier) recorded from HEK293 cells that were transiently transfected with the human cardiac calcium channel α_1 and rabbit α_2 are illustrated in Fig. 1 (*left*) or with the human α_1, rabbit α_2, and human β_3 subunits (Fig. 1, *right*). Voltage steps were applied from a holding potential of −100 mV to a test potential of +20 mV, at which the peak inward calcium currents were recorded. A major difference between the two subunit combinations was a severalfold increase in the calcium current magnitude with cotransfection of the β subunit.

As shown in the averaged current-voltage relationship (Fig. 2), both subunit combinations resulted in calcium channel currents that were activated at test potentials positive to −30 mV, and they reached a maximum near +20 mV. The peak current density was −3.9 ± 0.9 pA/pF for the α_1, α_2 subunit combination (n = 8) and −11.6 ± 2.2 pA/pF for the α_1, α_2, and β subunit combination (n = 9). The high-voltage activation threshold and the relatively slow inactivation of these currents identify them as being conducted through L-type calcium channels.

The voltage dependence for the activation of the calcium channel conductance (Fig. 3) was estimated by measuring the peak tail current amplitude (after subtraction of the gating current) after the repolarization of a brief test step (5.4 ms) to potentials of −80 through +80 mV (see inset for examples). For each cell, the absolute value of the corrected peak tail current amplitude was then normalized by the cell input capacitance (to yield pA/pF). Plots of the voltage dependence for the averaged calcium channel conductance for the two different subunit combinations (Fig. 3) revealed

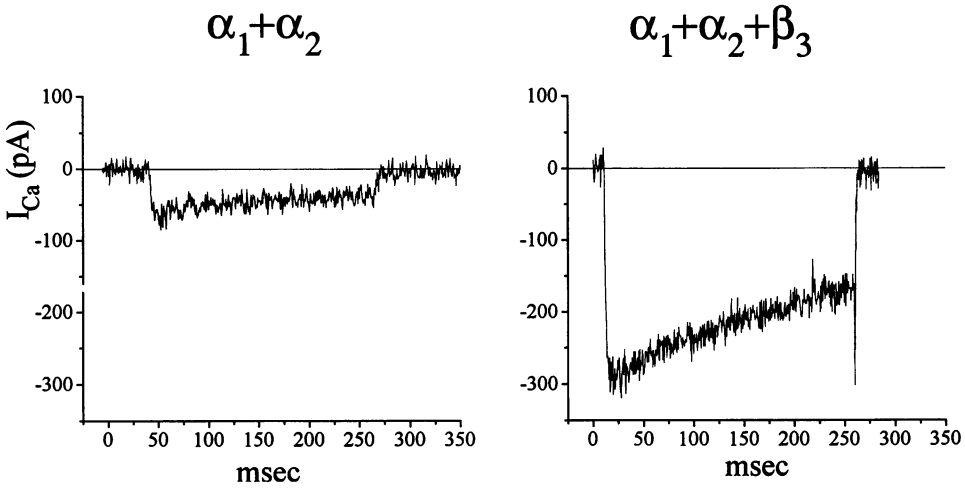

FIGURE 1 Calcium channel (ionic) currents recorded from HEK293 cells transfected with human cardiac L-type Ca channel subunits. (*Left*) (labeled $\alpha_1 + \alpha_2$) A Ca^{2+} current recorded after transfection with human α_1 and rabbit α_2 subunits. (*Right*) (labeled $\alpha_1 + \alpha_2 + \beta_3$) A Ca^{2+} current recorded after transfection with human α_1, rabbit α_2, and human β_3 subunits. Both currents were recorded from a holding potential of −100 mV, to a test voltage of +20 mV. The external solution contained 1.8 mM Ca^{2+} ions. The cell input capacitance was 22 pF and 24 pF for $(\alpha_1 + \alpha_2)$ and $(\alpha_1 + \alpha_2 + \beta_3)$.

that the β subunit increased the maximum average calcium channel tail current severalfold, from 8.6 ± 0.1 pA/pF (n = 10) to 32.1 ± 1.2 pA/pF (n = 14). Fig. 4 displays the same averaged data as Fig. 3, but each data set has been normalized to its maximum value, so that the voltage dependence for the activation of the conductances for the two subunit combinations may be directly compared. The voltage dependencies are quite similar, suggesting that the expression of the β subunit did not significantly alter the voltage dependence for calcium current activation.

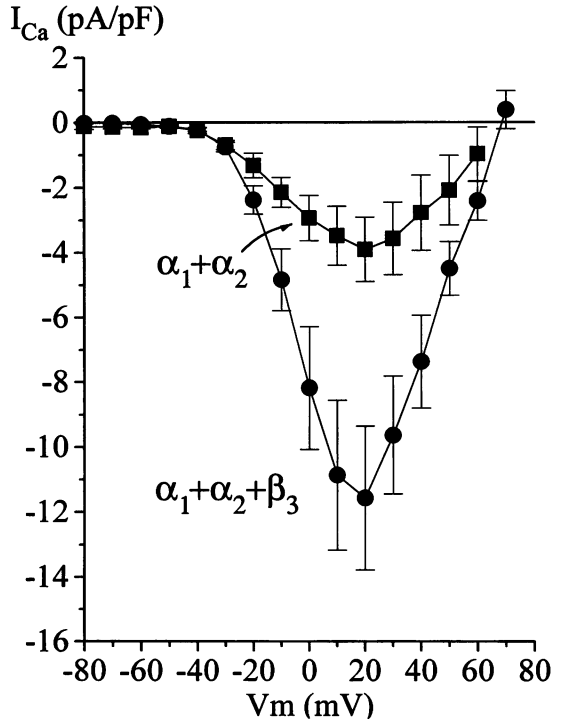

FIGURE 2 The current-voltage relationships for the peak inward L-type cardiac Ca^{2+} current density (pA/pF) recorded from HEK293 cells transfected with $\alpha_1 + \alpha_2$ subunits (■, n = 8), or $\alpha_1 + \alpha_2 + \beta_3$ subunits (●, n = 9). The mean Ca^{2+} current density ± SD is given; the data from each cell were normalized by the cell input capacitance.

It has previously been demonstrated that the single calcium channel current amplitude (i) is unchanged by the addition of the β subunit (Wakamori et al., 1993), which suggests that the expression of the β subunit increases the probability of Ca channel opening and/or the number of functional calcium channels. The following experiments provide evidence that supports the latter hypothesis.

Human cardiac calcium channel gating currents

Gating currents (nonlinear charge movements) were subsequently recorded from those HEK293 cells in which cardiac L-type Ca^{2+} currents were observed, after the addition of 5 mM Co^{2+} to the external solution and using the −P/5

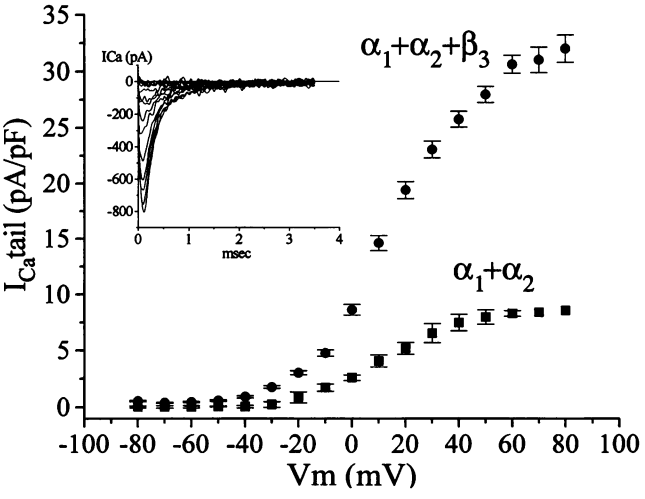

FIGURE 3 The voltage dependence for the conductance of human L-type cardiac Ca^{2+} channels composed of $\alpha_1 + \alpha_2$ subunits (■, n = 10), or $\alpha_1 + \alpha_2 + \beta_3$ subunits (●, n = 14). The conductance was estimated by measuring the peak tail currents after repolarization to −100 mV after 5.4-ms test steps. The OFF gating current was subtracted from the peak tail current amplitude. The resulting absolute value of the ionic tail current amplitude was normalized to the cell input capacitance before averaging. The inset shows examples of the time course of the tail currents ($\alpha_1 + \alpha_2 + \beta_3$ subunits) in response to voltage steps to −80 through +60 mV.

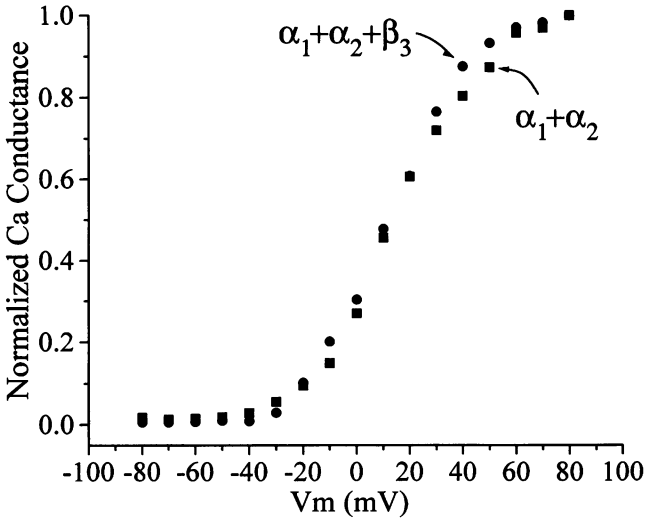

FIGURE 4 The normalized voltage dependence for the Ca^{2+} channel conductances. Same data as in Fig. 3, but each data set was normalized to its maximum value for comparison.

protocol for subtraction of the linear capacitive and leakage currents, as displayed in Fig. 5. As a control, no significant nonlinear charge movements could be recorded at any test potential from transfected cells that did not express L-type Ca currents, thus ruling out the possible contribution of other endogenous charge-sensing molecules in the membrane of HEK293 cells. In addition, it was necessary to set both the holding potential and the subtraction holding potential to −100 mV, so that the control subtraction currents would be obtained over a voltage region (i.e., negative to −100 mV) in which only linear capacity current was elicited. The linearity of the leakage currents in this subtraction voltage region is demonstrated in the inset of Fig. 5 *A*.

Fig. 5 *A* displays examples of a family of cardiac L-type Ca^{2+} channel gating currents recorded after transfection of HEK293 cells with human cardiac α_1 and rabbit α_2 subunits (Fig. 5 *A*, *left*) or after transfection with the human α_1, rabbit α_2, and human β subunits (Fig. 5 *A*, *right*). The gating currents were recorded at test potentials positive to −80 mV, at the onset of the test voltage step (IgON) and after the termination of the voltage step (IgOFF). Both IgON and IgOFF increased in magnitude with increasing test potential. The apparent rising phase of IgON was probably (at least in part) the result of the limited ability to instantaneously charge the cell membrane capacitance through the series resistance, although a true rising phase of the gating current cannot be ruled out at present. Nevertheless, the rapid activation of IgON always preceded the activation of the Ca^{2+} channel ionic currents.

In comparing the sets of gating currents displayed in Fig. 5 *A*, the most obvious feature is the severalfold increase in the current magnitude with the expression of the β subunit. The time course of individual gating currents at selected test potentials (with the β subunit) is shown in Fig. 5 *B*. Note that these currents decay to a zero baseline at the end of the voltage step, indicating the absence of either inward or outward ionic current contamination.

The amount of charge moved during the ON (QON, *filled circles*) and OFF (QOFF, *open circles*) components of the gating currents as a function of the test potential (QON-V_m and QOFF-V_m) is presented in Fig. 6. The gating current records from each cell were integrated (as described in Materials and Methods) to measure the amount of charge moved at each test potential, normalized to the cell input capacitance, and then averaged (expressed in units of nC/μF). Fig. 6 *A* displays QON and QOFF measured from the $\alpha_1 + \alpha_2$ cells, and Fig. 6, *B* and *C*, displays QON and QOFF with cotransfection of the β subunit.

A direct comparison of QON with QOFF is presented in Fig. 6 *C*. The means and the standard error bars of QON (*filled circles*) and the absolute value of QOFF (*open circles*) are plotted, and the symbols above the data indicate that these QON and QOFF values were not significantly different at the $p < 0.05$ (asterisks) or $p < 0.005$ (stars) level. The QON values were fit with a sum of two Boltzmann functions (*solid line*). In addition, also plotted are the 99% confidence levels of the Boltzmann fit. It is clear that, at all test potentials, QOFF was nearly equal to QON, so that there was a conservation of charge. This equality demonstrates that there was no immobilization of the Ca channel gating charge, as expected, given the brief pulse duration employed.

A comparison of the voltage dependence for the averaged QON data from the $\alpha_1 + \alpha_2$ and from the $\alpha_1 + \alpha_2 + \beta$ subunit combinations is presented in Fig. 7 *A*. When normalized to the cell capacitance, it is apparent that the averaged Q_{max} for the β-expressing cells (12.1 ± 0.3 nC/μF; $n = 8$) was severalfold larger than for $\alpha_1 + \alpha_2$ alone (2.5 ± 0.3 nC/μF; $n = 7$). Each of these QON data sets was then normalized to its Q_{max} value and plotted in Fig. 7 *B*. This figure demonstrates that the voltage dependence for QON was not substantially altered by the expression of the β subunit.

A fundamental mechanistic question that we wished to address in this study is the relationship between the activation of the gating charge movement and Ca^{2+} channel opening and ion conduction. The calcium channel conductance (G-V_m curve) was obtained by subtracting the OFF gating currents (recorded after the addition of Co^{2+}) from the total tail currents (ionic plus gating current) recorded before the addition of Co^{2+}. This step was necessary because the OFF calcium channel gating current was a significant fraction of the total tail current (see Hadley and Lederer, 1991), especially in these experiments using a low concentration of divalent charge carrier. The resulting calcium channel ionic tail currents were then normalized to the maximum ionic tail current. To compare the voltage dependence of the G-V_m curve with the QON-V_m curve the amount of surface charge shift produced by the additional divalent ion concentration (5 mM Co^{2+} ions), present in the charge movement experiments, was experimentally determined by comparison of the voltage dependence for the

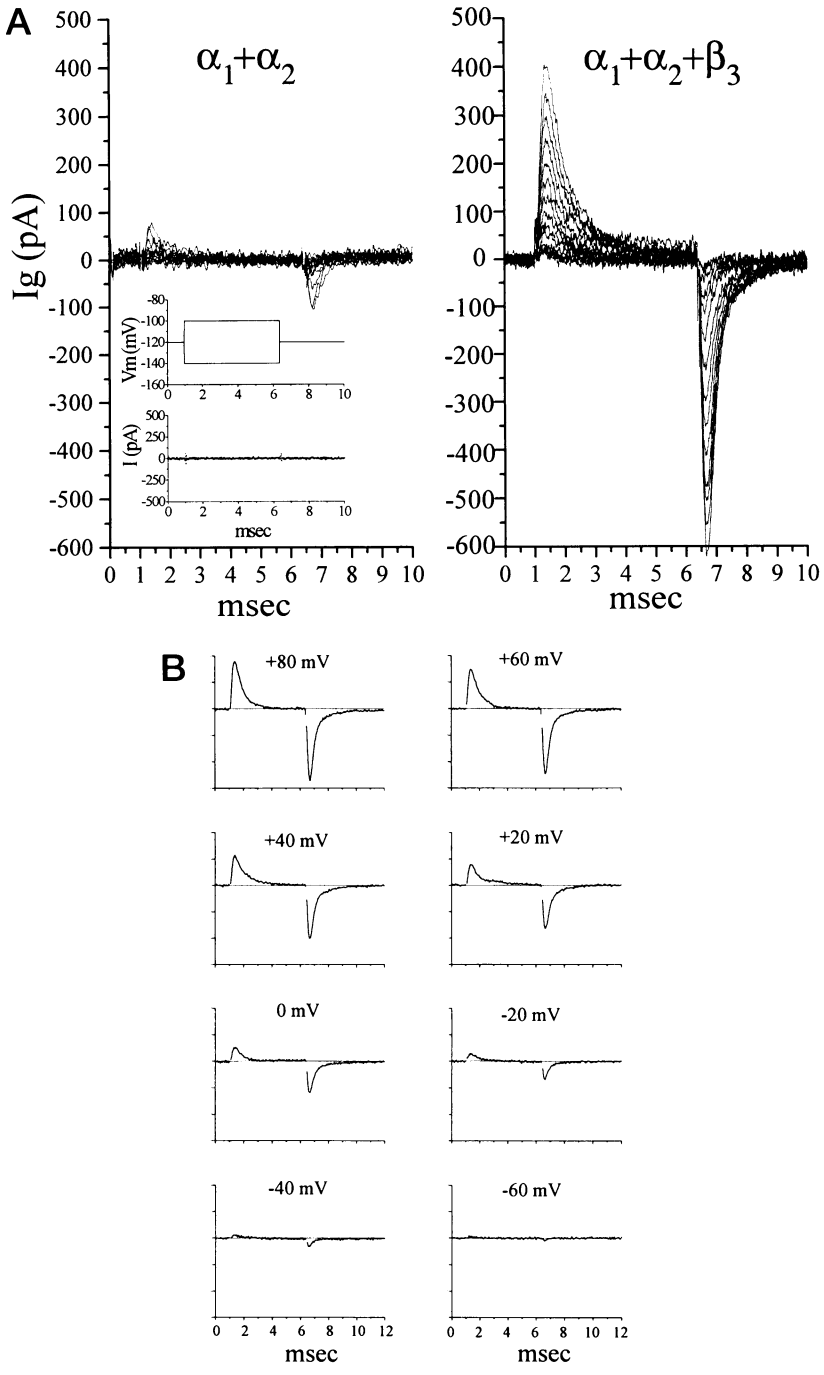

FIGURE 5 The gating currents (nonlinear charge movements) recorded from HEK293 cells transfected with human cardiac L-type Ca^{2+} channel subunits. In *A*, the left panel displays gating currents from a cell transfected with the human cardiac α_1 and rabbit α_2, alone (labeled $\alpha_1 + \alpha_2$). The right panel displays gating currents from a cell transfected with human cardiac L-type α_1, rabbit α_2, and human β_3 Ca^{2+} channel subunits (labeled $\alpha_1 + \alpha_2 + \beta_3$). As described in Materials and Methods, 5 mM Co^{2+} was used to block permeation through the Ca^{2+} channels, and the linear capacitance and leakage currents were subtracted by a $-P/5$ protocol. The holding potential was -100 mV, and test voltage steps were applied to -80 through $+60$ mV. The cell input capacitance was 25 pF and 35 pF for $(\alpha_1 + \alpha_2)$ and $(\alpha_1 + \alpha_2 + \beta_3)$. The inset (*left*) presents a demonstration of the linearity of the leakage currents. Voltage steps were applied to -100 mV and -140 mV from -120 mV (*top*), and the resulting currents summed to zero (below). (*B*) The time course of individual gating currents ($\alpha_1 + \alpha_2 + \beta$ subunits) at selected test potentials (-60 through $+80$ mV), as indicated. The current calibration is 250 pA/division.

peak amplitude and time course of the ON gating currents recorded before and after the administration of cobalt, and that value (+20 mV) was added to the G-V_m data to compensate for the shift. It was possible to employ this procedure only in cells with a very high channel expression in which large gating currents but relatively small Ca currents were recorded, perhaps due to Ca current rundown. In these cells, because of the relatively slow activation of a small-magnitude Ca current, the time course of the initial portion of the gating current was not obscured by the ionic current. An example of this procedure, applied over a wide range of potentials, is shown in Fig. 8 *A*. It was therefore possible to determine the surface charge shift produced by cobalt by comparing the peak magnitude and time course of the ON gating currents before and after cobalt.

A comparison of the voltage dependence for the activation of the charge movement (Q_{ON}-V_m curves, *closed circles*) with the voltage dependence for the activation of the Ca^{2+} conductance (G-V_m curves, *open circles*) is presented in Fig. 8. As displayed in Fig. 8 *B* ($\alpha_1 + \alpha_2$ subunits) and Fig. 8 *C* ($\alpha_1 + \alpha_2 + \beta$ subunits), the Ca^{2+} channel conductance was activated at test potentials positive to -20

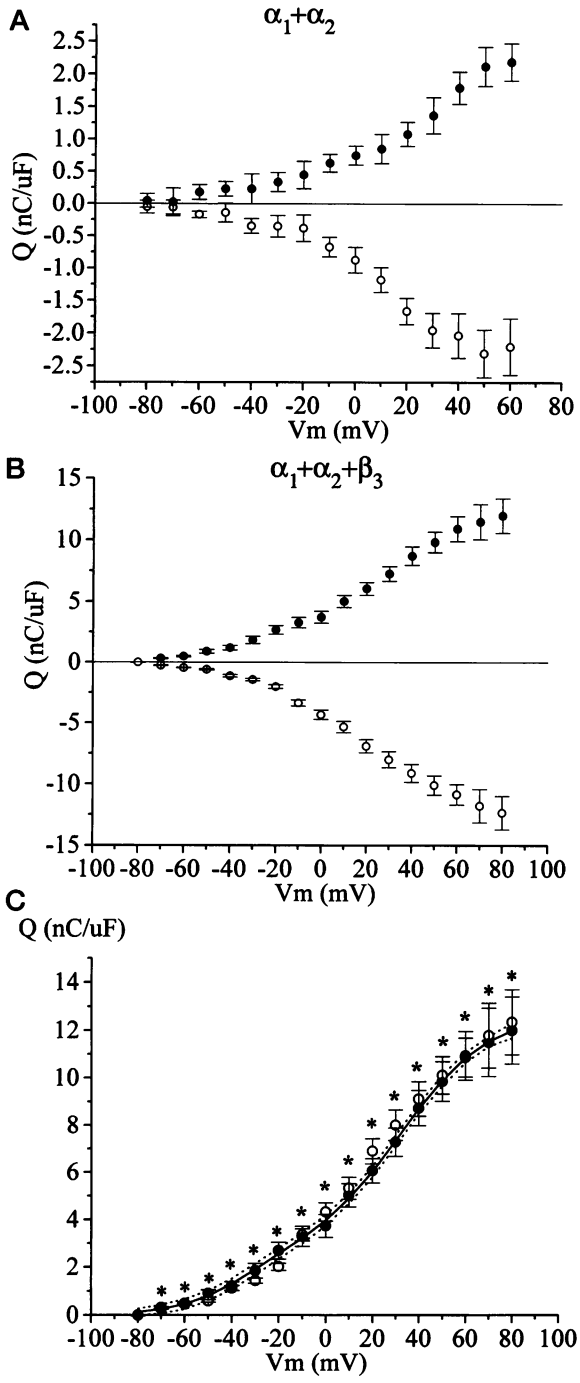

FIGURE 6 The QON-V_m and QOFF-V_m curves for the human cardiac L-type Ca^{2+} channels composed of $\alpha_1 + \alpha_2$ subunits (A, $n = 7$) and for the $\alpha_1 + \alpha_2 + \beta_3$ subunits (B and C; $n = 8$). QON and QOFF were obtained by integration of the ON (●) and OFF (○) Ca^{2+} channel gating currents. C is a plot of QON (●) and the absolute value of QOFF (○) for direct comparison. The mean QON data were fit (*solid line*) by a sum of two Boltzmann expressions, with the following parameters: $Q_{max}1$, 2.74 (0.82) nC/μF; $V1$, −34.8 (6.4) mV; $K1$, 14.3 (2.9) mV; and $Q_{max}2$, 9.96 (1.1) nC/μF; $V2$, 32.6 (2.4) mV; $K2$, 18.4 (2.2) mV. Also plotted are the 99% confidence limits for the Boltzmann fit (*dotted lines*). The asterisks and stars above each set of symbols indicate the statistical probabilities that the QON and QOFF are different; asterisks indicate $p < 0.05$, and stars indicate $p < 0.005$. In A, B, and C the charge data from each cell were normalized to the cell input capacitance and then averaged to give values in units of nC/μF. The data points are the means ± SE.

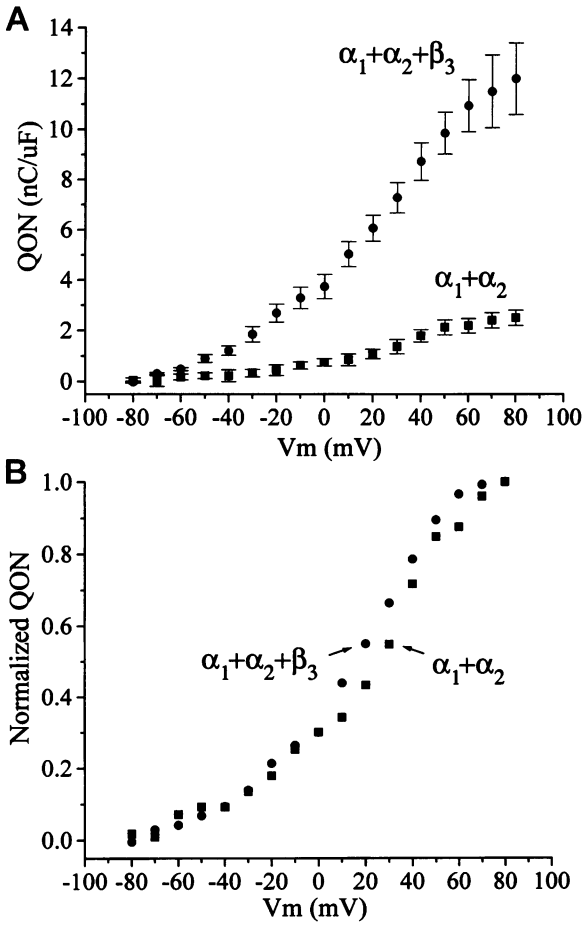

FIGURE 7 A comparison of the voltage dependence of QON for the $\alpha_1 + \alpha_2$ (■) and $\alpha_1 + \alpha_2 + \beta_3$ (●) subunit combinations. (A) Comparison of QON for the two subunit combinations. (B) Same data as shown in A, but each data set was normalized to its Q_{max} value.

mV, and its voltage dependence was well described by a single Boltzmann function. It is apparent that the G-V_m curve ranged over more positive potentials than did the Q_{ON}-V_m curve for both the $\alpha_1 + \alpha_2$ and the $\alpha_1 + \alpha_2 + \beta$ combinations. Moreover, a significant fraction of the total ON charge was activated at potentials more negative than those that activated the Ca^{2+} conductance. This finding suggests that at these negative potentials there was a voltage-dependent closed-state transition that did not result directly in Ca^{2+} channel opening and ion conduction. Furthermore, for both the $\alpha_1 + \alpha_2$ and $\alpha_1 + \alpha_2 + \beta$ subunit combinations the Q_{ON}-V_m data were better fit by a sum of two, rather than by a single Boltzmann function, suggesting that at least two distinct voltage-dependent processes contributed to Ca^{2+} channel activation. The apparent valences for these processes, derived from the steepness of each Boltzmann fit, were similar for the two components (~1.6 e^-) and for the two subunit combinations. However, for both subunit combinations, the charge component with the more negative voltage midpoint (−39 mV (B) and −32 mV (C)) included approximately one-quarter of the total charge,

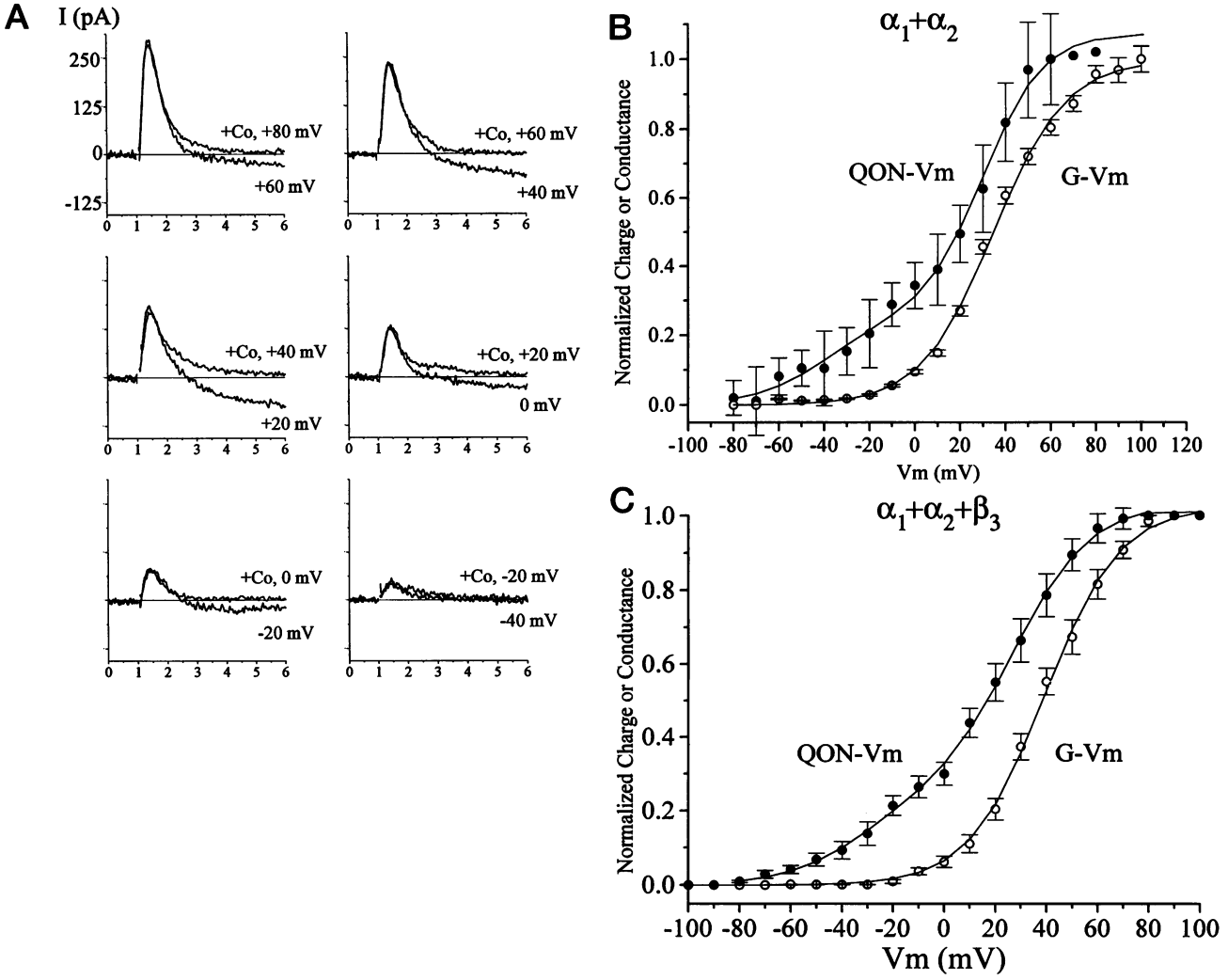

FIGURE 8 A comparison of the voltage dependence for the activation of the human L-type cardiac Ca^{2+} channel charge movement and conductance. (*A*) The method used to determine the amount of surface charge shift produced by the addition of 5 mM Co^{2+} in the charge movement experiments. Examples are shown of the superimposition of a family of gating currents recorded at +80, +60, +40, +20, 0, and −20 mV (after Co^{2+}, labeled +Co, *upper traces*) with the gating current plus calcium current traces in the same cell (Ig and ICa) at +60, +40, +20, 0, −20, and −40 mV (before Co^{2+}, *lower traces*); current and time calibrations: 125 pA/div, 1.0 ms/div. (*B* and *C*) The voltage dependence for the Ca channel charge movement (●) and for the Ca channel conductance (○) with the α_1 + α_2 (*B*) and with the α_1 + α_2 + β_3 subunits (*C*). The *G-V*$_m$ curve was shifted by +20 mV on the voltage axis to offset the surface charge shift produced by the 5 mM Co^{2+} used in the charge movement experiments. The calcium channel conductance was measured using a tail current method, after the subtraction of the OFF gating currents. The Boltzmann fits (*solid lines*) were calculated using the data from −80 to +80 mV and were drawn using the following parameters: for *A*: *G-V*$_m$: G_{max}, 1.0 (0.1); *V*, 34.5 (0.7) mV; *K*, 15.8 (0.6) mV; and for Q_{ON}-*V*$_m$: Q_{max1}, 0.25 (0.2); V_1, −38.8 (12.5) mV; K_1, 15.9 (3.5) mV; and Q_{max2}, 0.81 (0.1); V_2, 29.9 (1.1) mV; K_2, 13.1 (1.8) mV; for *B*: *G-V*$_m$: G_{max}, 1.0 (0.1); *V*, 39.1 (0.5) mV; *K*, 14.5 (0.4) mV; and for QON-*V*$_m$: Q_{max1}, 0.24 (0.1); V_1, −32.1 (12.2) mV; K_1, 15.7 (4.5) mV; and Q_{max2}, 0.79 (0.1); $V_{2,}$, 26.9 (3.3) mV; K_2, 15.1 (2.2) mV.

whereas the component with the more positive voltage midpoint (+30 mV (*B*) and +27 mV (*C*)) included approximately three-quarters of the total charge.

DISCUSSION

These results are the first demonstration of the properties of the gating currents (nonlinear charge movements) associated with the activation of cloned human cardiac L-type calcium channels expressed in a mammalian system. We found that the concomitant expression of the β subunit with the α_1 and α_2 subunits of the calcium channel not only increased calcium current density but also produced a fourfold augmentation of the amount of gating charge (Q_{max}) as compared to that produced by expression of the α_1 and α_2 subunits alone. This result may be interpreted to mean that the number of α_1 subunits expressed with functional gating and permeation properties was also increased to a comparable extent. In addition, the electrophysiological measurement of α_1 expression is consistent with previous findings of an increased binding capacity of dihydropyridine antagonists to the α_1 subunit of the calcium channel with the

coexpression of the β subunit (Varadi et al., 1991; Welling et al., 1993).

The present findings of β subunit-induced augmentation of human cardiac α_1 expression are in agreement with those obtained previously (Lory et al., 1993; Perez-Garcia et al., 1995) which demonstrated that the β subunit enhanced rabbit cardiac calcium channel currents expressed in mammalian cell lines. The present results using human heart calcium channels may also be compared to those reported previously (Neely et al., 1993) in which rabbit cardiac calcium channels were expressed, and gating and ionic currents were recorded using *Xenopus* oocytes. In the *Xenopus* oocyte expression system, the coexpression of the α_1 + β subunits did not increase the gating current Q_{max} above that obtained with the α_1 alone, although the calcium current density was increased severalfold (Neely et al., 1993). To explain these results the authors (Neely et al., 1993) suggested that the β subunit increased the coupling efficiency between the charge movement and calcium channel opening. Their interpretation also assumed that when the α_1 is expressed alone, a majority of the protein exists in a dihydropyridine-insensitive form. The latter postulation has not been substantiated by numerous studies (see Hofmann et al., 1994; Varadi et al., 1995 and references therein), although one recent study (Mitterdorfer et al., 1994) reports that the affinity of the α_1 for dihydropyridines increases by two orders of magnitude when coexpressed with the β subunit. However, the possibility remains that the differences in the findings of Neely et al. and the present work may be related to the different experimental conditions employed (e.g., the presence of the α_2 subunit and the mammalian expression system employed). In the present results, the increase in calcium current density by β subunit expression appears to be a direct result of an increase in Q_{max} (number of functional calcium channel α_1 proteins), although an additional effect of the β subunit on the coupling between charge movement and channel opening may also contribute to some extent. Our gating current data are also consistent with those presented in a preliminary report by Kamp et al., using rabbit cardiac α and β subunits (Kamp et al., 1995, abstract).

There are several advantages in using the HEK293 expression system for the present experiments. First, the calcium channel gating currents can be studied in isolation, without additional procedures to eliminate the gating charge movements of other types of channels. For example, in native cardiac myocytes charge movements from Na^+ channels must be separated from those of calcium channels on the basis of steady-state (Bean and Rios, 1989; Hadley and Lederer, 1989, 1991; Josephson and Sperelakis, 1992), kinetic (Josephson and Sperelakis, 1992; Josephson and Cui, 1995), or pharmacological (Josephson and Cui, 1994) methods. Second, the HEK293 is a mammalian cell line, so that its genetic machinery and posttranslational processing more closely match a human heart cell than does the *Xenopus* oocyte expression system. Third, we can select which calcium channel subunits we wish to express, so that we are able to study the effects of the expression of specific calcium channel subunit combinations. Fourth, we can study calcium channel currents using the physiological cation calcium, because calcium-activated chloride currents (present in *Xenopus* oocytes) are absent.

It is widely believed that the highly conserved, positively charged S4 segments of domains I–V of the α_1 subunit of Na^+, Ca^{2+}, and K^+ channels are involved in the voltage-sensing function of these membrane proteins (Catterall, 1988). The present results reveal that there are two distinct components of the steady-state charge movement of human L-type Ca^{2+} channels, one with a more negative voltage midpoint composing approximately one-fourth of the total charge, and the other with a more positive voltage midpoint composing approximately three-fourths of the total charge. It is very tempting to speculate that the more negative voltage component may arise from the movement (i.e., a voltage-driven conformational change) of one of the S4 segments, and that the more positive voltage component may arise from the movements of the three other S4 segments. If we assume in the simplest case that all of the S4 segments are equivalently charged it may be possible that one of the S4 segments "senses" a different local environment, due to a difference in the charge groups of surrounding structures, and may therefore be more easily mobile (i.e., over a lower voltage range) than the other S4s. Another possibility is the presence of cooperative or allosteric interactions between the different S4 segments and/or motifs. Thus the movement of the first, lower-voltage S4s may somehow alter the environment and energy barriers that the other S4 segments "sense," thereby shifting their voltage dependence to more positive potentials. Further gating current exploration will be necessary to determine which, if either, of these models is closer to the actual gating mechanism leading to Ca^{2+} channel opening.

The authors thank Dr. Arnold Schwartz for his support and encouragement of the work, for helpful discussions, and for critiquing the manuscript. We also thank Dr. Gabor Mikala for providing the Hb_3 for these studies and Marie Varadi for her excellent technical assistance.

This work was supported by National Institutes of Health HL-45624 (IJ), by National Institutes of Health HL-43321 and HL-22629 (AS), and by a grant from the Tanabe Seiyaku Co. for Molecular Pharmacology and Biophysics.

REFERENCES

Bean, B. P., and E. Rios. 1989. Nonlinear charge movement in mammalian cardiac ventricular cells. *J. Gen. Physiol.* 94:65–93.

Catterall, W. A. 1988. Structure and function of voltage-sensitive ion channels. *Science.* 242:50–61.

Chen, C., and H. Okayama, H. 1987. High-efficiency transformation of mammalian cells by plasmid DNA. *Mol. Cell. Biol.* 7:2745–2752.

Collin, T., P. Lory, S. Taviaux, C. Courtieu, P. Guilbault, P. Berta, and J. Nargeot. 1994. Cloning, chromosomal location and functional expression of the human voltage-dependent calcium channel b3 subunit. *Eur. J. Biochem.* 220:257–262.

De Waard, M., M. Pragnell, and K. P. Campbell. 1994. Calcium channel regulation by a conserved β subunit domain. *Neuron.* 13:495–503.

Ellis, S. B., M. E. Williams, N. R. Ways, R. Brenner, A. H. Sharp, A. T. Leung, K. P. Campbell, E. McKenna, W. J. Koch, A. Hui, A. Schwartz, and M. M. Harpold. 1988. Sequence and expression of mRNAs encoding the α_1 and α_2 subunits of a DHP-sensitive calcium channel. *Science.* 241:1661–1664.

Hadley, R. W., and W. J. Lederer. 1989. Intramembrane charge in guinea-pig and rat ventricular myocytes. *J. Physiol. (Lond.)* 415:601–624.

Hadley, R. W., and W. J. Lederer. 1991. Properties of L-type Ca channel gating currents in isolated guinea-pig ventricular myocytes. *J. Gen. Physiol.* 98:265–285.

Hamill, O. P., A. Marty, E. Neher, B. Sakmann, and F. J. Sigworth. 1981. Improved patch-clamp techniques for high-resolution current recording from cells and cell-free membrane patches. *Pflugers Arch.* 391:85–100.

Hofmann, F., M. Biel, and V. Flockerzi. 1994. Molecular basis of Ca channel diversity. *Annu. Rev. Neurosci.* 17:399–418.

Isom, L., K. DeJongh, and W. A. Catterall. 1994. Auxiliary subunits of voltage-gated ion channels. *Neuron.* 12:1183–1194.

Josephson, I. R., and Y. Cui. 1994. Voltage- and concentration-dependent effects of lidocaine on cardiac Na channel and Ca channel gating charge movements. *Pflugers Arch.* 428:485–491.

Josephson, I. R., and Y. Cui. 1995. Cardiac gating charge movements: recovery from inactivation. *Pflugers Arch.* 430:682–689.

Josephson, I. R., and N. Sperelakis. 1992. Kinetic and steady-state properties of Na^+ channel and Ca^{++} channel charge movements in ventricular myocytes of embryonic chick heart. *J. Gen. Physiol.* 100:195–216.

Kamp, T. J., M. T. Perez-Garcia, and E. Marban. 1995. Coexpression of β subunit with L-type calcium channel α_{1C} subunit in HEK293 cells increases ionic and gating currents. *Biophys. J.* 68:A349.

Klockner, U., G. Mikala, M. Varadi, G. Varadi, and A. Schwartz. 1995. Involvement of the carboxyl-terminal region of the α_1 subunit in voltage-dependent inactivation of cardiac calcium channels. *J. Biol. Chem.* 270:17306–17310.

Kuniyasu, A., K. Oka, A. Ide-Yamada, T. Hatakana, T. Abe, H. Nakayama, and T. Kanaoka. 1992. Structural characterization of the dihydropyridine-linked calcium channel from porcine heart. *J. Biochem. (Tokyo).* 112:235–242.

Lory, P., G. Varadi, D. Slish, M. Varadi, and A. Schwartz. 1993. Characterization of the beta subunit modulation of a rabbit cardiac L-type Ca channel α_1 subunit as expressed in mouse L cells. *FEBS Lett.* 315: 167–172.

Mitterdorfer, J., M. Froschmayr, M. Grabner, J. Striessnig, and H. Glossman. 1994. Calcium channels: the β subunit increases the affinity of dihydropyridine and Ca^{2+} binding sites of the α_1 subunit. *FEBS Lett.* 352:141–145.

Miyazaki, J., S. Takaki, K. Araki, F. Tashiro, A. Tominaga, K. Takatsu, and K. Yamamura. 1989. Expression vector system based on the chicken a-actin promoter directs efficient production of interleukin-5. *Gene.* 79:269–277.

Neely, A., X. Wei, R. Olcese, L. Birnbaumer, and E. Stefani. 1993. Potentiation by the β subunit of the ratio of the ionic current to the charge movement in the cardiac calcium channel. *Science.* 262:575–578.

Perez-Garcia, M., T. Kamp, and E. Marban. 1995. Functional properties of cardiac L-type calcium channels transiently expressed in HEK293 cells. *J. Gen. Physiol.* 105:289–306.

Pragnell, M., M. De Waard, Y. Mori, T. Tanabe, T. P. Snutch, and K. P. Campbell. 1994. Calcium channel β-subunit binds to a conserved motif of the I-II cytoplasmic linker of the α_1 subunit. *Nature.* 368:67–70.

Sanes, J. R., J. L. R. Rubenstein, and J.-F. Nicolas. 1986. Use of recombinant retrovirus to study post-implantation cell lineage in mouse embryos. *EMBO J.* 5:3133–3142.

Schultz, D., G. Mikala, A. Yatani, D. B. Engle, D. E. Iles, B. Segers, R. J. Sinke, D. Olde Weghuis, U. Klöckner, M. Wakamori, J.-J. Wang, D. Melvin, G. Varadi, and A. Schwartz. 1993. Cloning, chromosomal localization and functional expression of the α_1 subunit of the L-type voltage-dependent calcium channel from normal human heart. *Proc. Natl. Acad. Sci. USA.* 90:6228–6232.

Varadi, G., P. Lory, M. Schultz, M. Varadi, and A. Schwartz. 1991. Acceleration of activation and inactivation by the β subunit of the skeletal muscle Ca channel. *Nature.* 352:159–162.

Varadi, G., Y. Mori, G. Mikala, and A. Schwartz. 1995. Molecular determinants of Ca channel function and drug action. *Trends Pharmacol. Sci.* 16:43–49.

Wakamori, M., G. Mikala, A. Schwartz, and A. Yatani. 1993. Single-channel analysis of a cloned human heart L-type Ca channel α_1 subunit and the effects of a cardiac β subunit. *Biochem. Biophys. Res. Commun.* 196:1170–1176.

Welling, A., E. Bosse, A. Cavalie, R. Bottlender, A. Ludwig, V. Flockerzi, and F. Hofmann. 1993. Stable co-expression of calcium channel α_1, b, and α_2d subunits in a somatic cell line. *J. Physiol. (Lond.)* 471:749–765.